Optimising Femtocell Placement in an Interference Limited Network: Theory and Simulation

Siyi Wang, Weisi Guo, Tim O'Farrell
Department of Electronic and Electrical Engineering
The University of Sheffield, Mappin Street, Sheffield, S1 3JD, United Kingdom
{siyi.wang, w.guo, t.ofarrell}@sheffield.ac.uk

***Abstract*—The purpose of this paper is to show that the indoor downlink capacity and energy efficiency can be significantly improved by optimising the indoor location of femtocell. This body of investigation is done in the presence of outdoor interference and the simulation results are backed up by a novel theoretical framework employing convex optimisation. Moreover, this optimisation problem has been demonstrated to be meaningful in the context of considering capacity saturation of realistic modulation and coding schemes. The results yield insight into the relationship between the outdoor and indoor aspects of the cellular network, as well as the propagation parameters. The paper shows that a mean capacity improvement of up to 20% can be made with optimal placement, which translates to an operational energy reduction of 8%. Moreover, it has been shown that the optimisation does not significantly degrade the performance of outdoor network. The global impact of this work is that 1.6 TWh can be saved globally, which amounts to the energy produced by two 1000 MW power plants.**

I. Introduction

In recent years, data traffic has experienced a 10 fold growth and the associated energy consumption has increased by up to 20%. Demand for higher data rates has created new challenges for cellular operators. One of the challenges is delivering high traffic rates to indoor users where there is typically insufficient cellular coverage. Femtocell Access Points (FAP) have attracted significant attention as a solution to increase the system capacity of wireless networks [1]. One challenge that remains unsolved is where to locate an indoor FAP in the presence of outdoor micro-cell interference. Conventionally, FAPs are likely to be placed near walls and corners where it is convenient and situated close to a power source. This paper shows that a FAP's position can significantly affect the system capacity and energy consumption, and it is not intuitively obvious where it should be placed. For a given amount of data transmitted, the higher the femtocell capacity, the lower the transmission time. This can also be translated to an radio-head (RH) energy reduction, which can be extended to the operational (OP) energy reduction by considering a fixed overhead (OH) power consumption. The energy consumption can be reduced to a lower-bound of the ratio between the OH power and the OP power, which is about 80%.

A. Challenges and Proposed Solution

As far as we know, the challenge of FAP placement remains an open challenge. Most existing work assumes that the coverage of the FAP is of a fixed radius and that there are a fixed number of users are at fixed locations around the FAP [2]–[4]. Most existing work has concentrated on managing the transmitting power and radio resource management between the FAP and the outdoor cell-site [5]–[7]. Moreover, most existing work do not have a theoretical framework for validation. Such techniques can be integrated into the optimal placement solution we propose.

In contrast with previous research, this paper optimises the FAP indoor position with the aim of achieving the highest mean capacity, in the presence of co-channel interference from an outdoor base station. This is done with the aid of simulation results and a novel theoretical framework. The analytical approach is corroborated by means of a Monte Carlo simulation which encapsulates sub-carrier level interference and user mobility modelling. The remainder of the paper is organised as follows. In Section II, the system level of LTE-femtocell simulator is described, which is followed by the detailed description of the proposed theoretical algorithm in Section III. The simulation results of capacity along with the associated energy reduction performance and discussions are given in Section IV. Section V concludes the whole paper. Full derivation of the theoretical framework can be found in the Appendix.

II. System Model

A. Introduction

An LTE system level simulator has been developed to optimise the FAP placement for an enterprise office area. Fig. 1(a) and Fig. 1(b) illustrate the system model and the average received SINR of such a deployment. A number of users are randomly and evenly distributed within the office area and their mean downlink throughput is considered as the characteristic metric for optimisation. Only one single rectangular room without internal light walls is considered. We consider 1 FAP with 1 outdoor micro-cell as interference. The assumptions made are:

- The micro-cell is the dominant interference source to the FAP, because most FAPs are likely to be within the coverage area of a single cell-site.
- The micro-cell is fully loaded and persistently interfere with the FAP.

978-1-4673-1881-5/12/$31.00 ©2012 IEEE

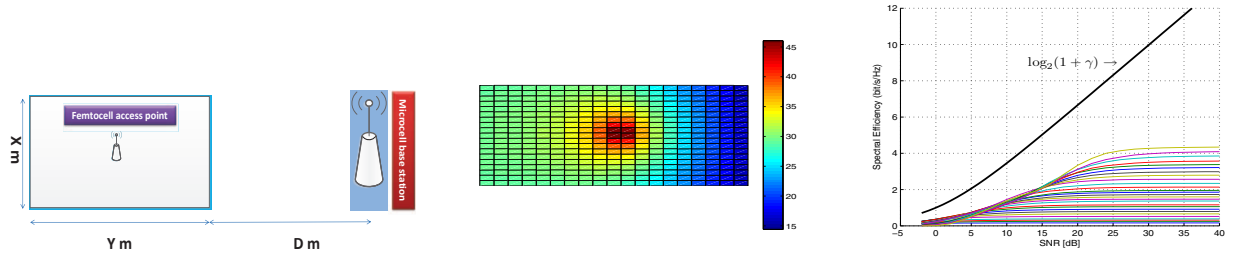

(a) Simulation and theoretical model (b) SINR grid map (c) Throughput vs. SNR WINNER_II A1 SISO

Fig. 1. Simulation and theoretical model

- The effect of FAP interference on the micro-cell is not considered in this body of investigation as it only concerns indoor coverage.

The path loss models implemented in the simulator are adopted from WINNER A1 and B4 [8]. The indoor path loss model PL_{in} (between the FAP and the mobile user) and the outdoor-to-indoor $\text{PL}_{\text{out-to-in}}$ (between the micro-cell base station and the mobile user) are defined as follows, respectively:

$$\text{PL}_{\text{in}} = 18.7\log_{10}\left(d_{\text{FAP}}\right) + 46.8 + 20\log_{10}\left(\frac{f}{5}\right), \quad (1)$$

$$\begin{aligned}\text{PL}_{\text{out-to-in}} =& 36.7\log_{10}\left(d_{\text{micro}}\right) + 22.7 + 26\log_{10}\left(\frac{f}{5}\right) \\ &+ \text{PL}_{\text{wall}} + 0.5d_{\text{in}},\end{aligned} \quad (2)$$

where f is frequency of transmission in GHz. d_{FAP}, d_{micro} and d_{in} are FAP-to-user, micro-cell-to-user and wall-to-user distance in metres. PL_{wall} is the wall loss penetration factor in dBs.The received Signal to Interference-plus-Noise Ratio (SINR) is calculated as below:

$$\gamma = \frac{|h_0|^2 P_0}{|h_k|^2 P_k + \sigma^2}, \quad (3)$$

where h_0 and $h_k \sim \mathcal{CN}(0,\ 1)$ are the multi-path coefficient of the FAP and micro-cell base station, respectively. They are modelled as independent and identically distributed (i.i.d.) circularly symmetric complex Gaussian random variables with zero mean and a variance of one. P_0 is the received power of one sub-carrier from the FAP, P_k is the received power of the same sub-carrier from the micro-cell base station and σ^2 is the noise power. Without considering radio resource management techniques, the paper considers a round-robin scheduler, which evenly partitions the resource blocks between users.

B. Simulation Framework

In the simulation framework, the FAP location is varied across the room. For each location, a sufficiently high number of user positions are considered to yield converging results of the network mean capacity. The traditional brute-force exhaustive grid-search is employed to find the optimal FAP placement that yields the highest mean user throughput. The simulator supports link adaptation by changing the Modulation and Coding Scheme (MCS) based on the channel quality (i.e., SINR). The link level MCS is generated from the Vienna LTE simulator [9] under the WINNER II A1 multipath model [8]. The corresponding throughput versus Signal to Noise Ratio (SNR) curves of the look-up tables are illustrated in Fig. 1(c).

III. Theoretical Framework

A. Introduction

In order to verify the simulation result of the optimal coordinate for a FAP to maximise the mean throughput in a particular office, an extensive theoretical model to solve this optimal problem has been developed under certain assumptions. Those assumptions are as follows:

- The throughput experienced by indoor users are always in the high SINR regime, and that at least some region of the room experiences saturated throughput. This has been verified to be accurate after extensive simulation runs.
- The variation of throughput is mainly along the axis of the FAP-Microcell, and not orthogonal to it.
- A modified Shannon expression is used for throughput, which accounts for the mutual information saturation of modulation and coding schemes.

In a rectangular office with Cartesian co-ordinates of x and y, $\gamma_{x,y}$ is defined as the received SINR for a user at a particular position can be expressed in (4), where $\frac{P_{\text{FAP}} D^{3.67} \times 10^{(22.7+\text{PL}_{\text{wall}})/10} \times (\frac{f}{5})^{2.6}}{P_{\text{micro}} \overline{G}_{\text{micro}} \times 10^{46.8/10} \times (\frac{f}{5})^2}$ is denoted as K_γ, $\alpha = 1.87$ and $\beta = 0.05$. P_{FAP} and P_{micro} are the transmitting power of FAP and micro-cell station, respectively. $\overline{G}_{\text{micro}}$ is the expected value of the antenna gain from the micro-cell base station. $d_{x,y,\text{FAP}}$ is the i^{th} FAP-to-grid distance and $d_{x,y,\text{micro}}$ is the i^{th} micro-cell-to-grid distance. $d_{x,y,\text{in}}$ is the distance between the wall and i^{th} grid. As $D \gg d_{x,y,\text{in}}$, $d_{x,y,\text{micro}}$ can be accurately estimated as D. $\gamma_{x,y}$ can then be re-written as $\boldsymbol{K_\gamma \frac{10^{\beta d_{x,y,\text{in}}}}{d_{i,\text{FAP}}^{\alpha}}}$.

For a given FAP position of $(x = a, y = b)$, the mean capacity of users attached to this FAP is therefore:

$$\begin{aligned}\overline{C}_{a,b} &\approx \frac{1}{A}\iint_A \log_2(\gamma_{x,y})\ \mathrm{d}x\,\mathrm{d}y, \\ &= \frac{1}{A}\iint_A \log_2\left[K_\gamma \frac{10^{\beta|y|}}{\left(\sqrt{(x-a)^2 + (y-b)^2}\right)^{\alpha}}\right]\ \mathrm{d}x\,\mathrm{d}y.\end{aligned} \quad (5)$$

$$\gamma_{x,y} = \frac{\frac{P_{\text{FAP}}}{(d_{x,y,\text{FAP}})^{1.87}\times 10^{46.8/10}\times(\frac{f}{5})^2}}{\frac{P_{\text{micro}}\overline{G}_{\text{micro}}}{(d_{x,y,\text{micro}})^{3.67}\times 10^{(22.7+\text{PL}_{\text{wall}}+0.5d_{x,y,\text{in}})/10}\times(\frac{f}{5})^{2.6}}+\sigma^2} \approx \frac{P_{\text{FAP}}D^{3.67}\times 10^{(22.7+\text{PL}_{\text{wall}})/10}\times(\frac{f}{5})^{2.6}}{P_{\text{micro}}\overline{G}_{\text{micro}}\times 10^{46.8/10}\times(\frac{f}{5})^2}\frac{10^{\beta d_{x,y,\text{in}}}}{d^{\alpha}_{x,y,\text{FAP}}}. \quad (4)$$

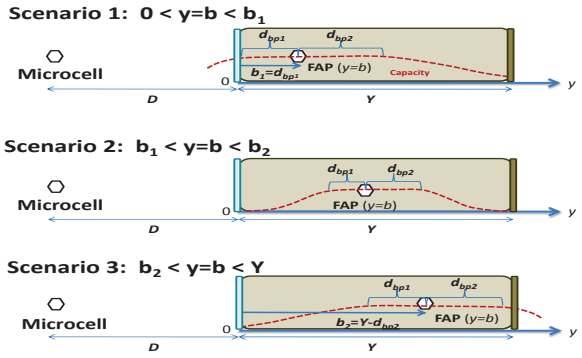

Fig. 2. Illustration of the analytical scenarios with respect to the saturated capacity region with respect to different FAP positions inside the room.

As it can be noted from Fig. 1(b), $\gamma_{x,y}$ (15–45 dB) is much greater than 1 which makes the above high SINR approximation reasonable. According to the MCS table, the throughput will saturate when $\gamma_{x,y} > \gamma_s = 35.94$ dB, **where γ_s is the saturation SNR threshold**. Hence, $\overline{C}_{a,b}$ should be modified to reflect this saturated region, which is shown as d_{bp1} and d_{bp2} in Fig. 2. It is also worth pointing out that $\gamma_{x,y}$ hardly fluctuates along x axis outside the saturated region. Eq. (5) can be re-written as Eq. (6) for simplicity of theoretical analysis yet without loss of generality:

$$\overline{C}^b = C_{\text{s}}Y_{\text{s}} + \frac{1}{Y_{\text{ns}}}\int_{Y_{\text{ns}}} \log_2\left(K_\gamma \frac{10^{\beta y}}{|y-b|^{\alpha}}\right) \text{d}y, \quad (6)$$

where $C_{\text{s}} = \log_2(1+10^{\frac{\gamma_{\text{s}}}{10}})$ bit/s/Hz. Y_{s} and Y_{ns} are the length of saturated and non-saturated regions, respectively. Eq. (6) can be split into three sub-functions with respect to FAP position b. (Proof can be found in the Appendix). The final expression of the mean capacity of the network with respect to the position of the FAP b is as follows:

$$\overline{C}^b = \begin{cases} P_1 + Q_1 + R_1 - \frac{\alpha}{Y}(T_1 - U_1), & 0 < b \leqslant b_1 \\ P_2 + Q_2 + R_1 + R_2 & \\ -\frac{\alpha}{Y}(T_1 + T_2 - U_1 - U_2), & b_1 < b \leqslant b_2 \\ P_3 + Q_3 + R_2 - \frac{\alpha}{Y}(T_2 - U_2), & b_2 < b < Y \end{cases} \quad (7)$$

It can be shown that the function is convex and that according to the first rule of finding the maximum value of a function, stationary points can be determined by differentiating Eq. (7) (Note: $\frac{\partial d_{bp1}}{\partial b} = \frac{B\exp[-W(F)]\ln 10}{20\alpha[1+W(F)]}$ and $\frac{\partial d_{bp2}}{\partial b} = \frac{B\exp[-W(-F)]\ln 10}{20\alpha[1+W(-F)]}$) and then solving the differentiated function for zeros. The resulting expression is a closed form expression, but is unfortunately too long for the scope of this paper. All the stationary points are tested in order to verify the type of the stationary points (max) by checking if the corresponding value in the second-order differential function of Eq. (7) is negative. Finally, the mean capacity value(s) corresponding to all the stationary points are compared with all endpoints of the interval of each sub-function in Eq. (7) and the global maximum value is selected as the maximum of mean capacity. The solution b_{opt} is the optimal coordinate for FAP placement. The following section will illustrate both the simulation and the theoretical results.

IV. Simulation and Theoretical Results

The optimal placement is judged according to salient system variables: the micro-cell base station location, the material of the wall and the ratio of micro-cell and FAP transmitting power. A baseline conventional FAP deployment has been considered. FAP is placed at the corner of the room where the power socket is typically located. The result of the capacity difference between the optimal and the conventional is illustrated in the sub-plots of Fig. 3, Fig. 4 and Fig. 5. The theoretical results are shown in lines and are compared with the simulation results shown as symbols. The parameters used in the investigation are as follows: Office size (10 × 20 m), System bandwidth (20 MHz), Carrier frequency (2130 MHz), Total number of users (10), Sub-carriers per Physical Resource Block (12), FAP transmitting power (0.01–0.1 W), micro-cell transmitting power (5–40 W), FAP radio-head efficiency (6.67%), FAP overhead power (5.2 W), Micro-cell distance away from the office (150–450 m), and Wall loss (0–20 dB).

A. Capacity Results

The impact of the micro-cell to office distance D on the performance of finding the optimal position is shown in Fig. 3, when $\text{PL}_{\text{wall}} = 10$ dB, $P_{\text{FAP}} = 0.1$ W and $P_{\text{micro}} = 20$ W. The influence of the wall penetration loss is depicted in Fig. 4 when $D = 200$ m, $P_{\text{FAP}} = 0.1$ W and $P_{\text{micro}} = 20$ W. And Fig. 5 shows the power ratio of micro-cell to FAP base station effect on the optimal placement decision.

The users in the office suffer the most severe interference from the outdoor micro-cell (i.e. $D = 150$ m in Fig. 3, $\text{PL}_{\text{wall}} = 0$ dB in Fig. 4 and power ratio = 1000 in Fig. 5), the optimal position tends to be in the middle of the enterprise office. This position steadily moves towards the micro-cell direction and converges to approximately 5–6 m away from the wall close to the micro-cell base station. The black curves in the optimal coordinate plots provide an accurate match to the results obtained from the simulator. The mean capacity difference between the optimal FAP position and the worst position (i.e. the smallest mean capacity) is illustrated in the lower half of Fig. 3, Fig. 4 and Fig. 5. The worst position is always at the corner of the far ending of the office. It can be seen that the capacity difference calculated both in

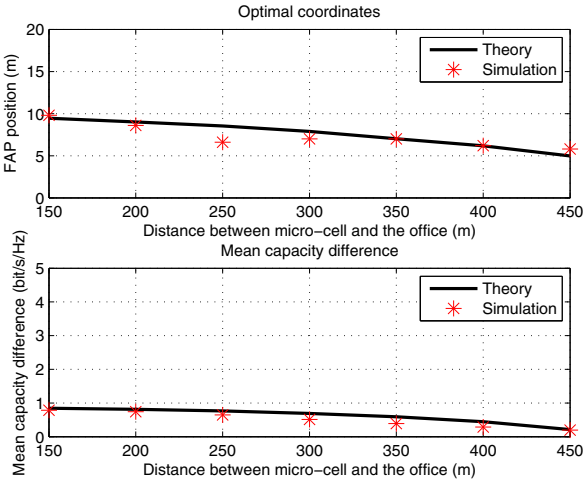

Fig. 3. Impact of distance between micro-cell and the office

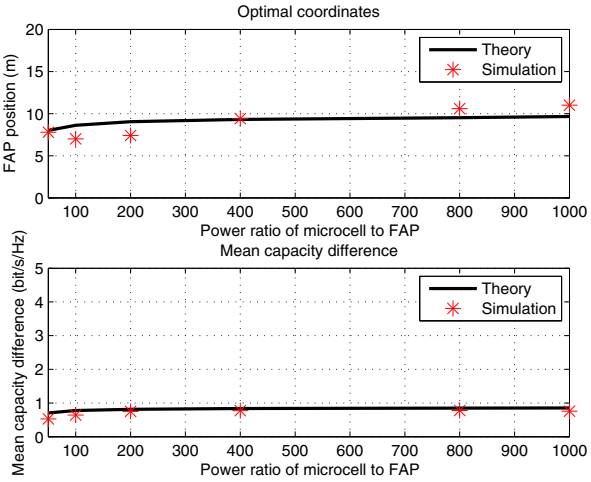

Fig. 5. Power ratio of microcell to FAP

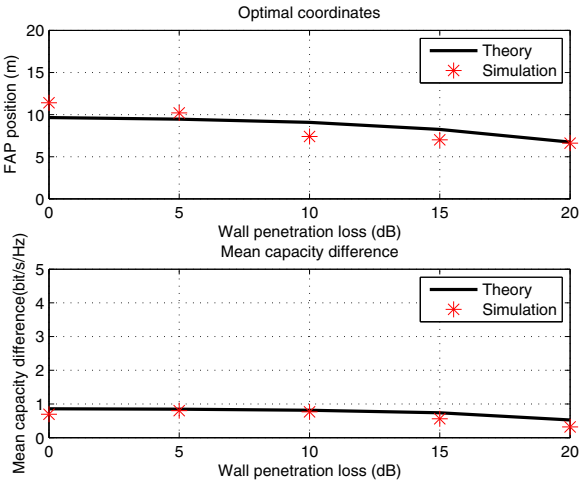

Fig. 4. Wall penetration loss effect

theoretical model by Shannon's Capacity equation and the simulation from an MCS look-up table is between 0.2 bit/s/Hz and 0.8 bit/s/Hz. The following section will describes how much operational (OP) energy can be saved for an optimal FAP position compared to the worst scenario.

It can be noted that our solution of optimising the FAP location does not significantly degrade the outdoor network performance. By moving the FAP from 0 to 5 m closer to the cell-site, the interference to the outside network is increased by 0-2.5 dB, compared to when the FAP is placed in middle of the room. When compared to the FAP randomly placed, the interference is not significantly increased.

B. Energy Results

In order to compare the energy consumption of the same system operating in different conditions, the concept of transmission duration and operational duration are defined. Consider a FAP with indoor users that demand a traffic load of M bits of data over a finite time duration of $T_{\text{FAP}}^{\text{OH}}$. Two systems are considered: a reference and a test system, both of which have a capacity that exceed the offered traffic load. Due to the fact that the reference and the test system might have different capacities and scheduling mechanisms, the duration which the radio-head spends in transmitting the same M bits is different. In order to compare two systems, useful metric is the Energy Reduction Gain (ERG), which is the reduction in energy consumption when a test system is compared with a reference system:

$$\begin{aligned}\text{ERG}_{\text{RAN}}^{\text{OP}} &= 1 - \frac{E_{\text{FAP,test}}^{\text{OP}}}{E_{\text{FAP,ref.}}^{\text{OP}}} \\ &= 1 - \frac{P_{\text{test}}^{\text{RH}} \frac{R_{\text{traffic}}}{R_{\text{FAP,test}}} + P_{\text{test}}^{\text{OH}}}{P_{\text{ref.}}^{\text{RH}} \frac{R_{\text{traffic}}}{R_{\text{FAP,ref.}}} + P_{\text{ref.}}^{\text{OH}}},\end{aligned} \tag{8}$$

where $P_i^{\text{RF}}/\mu_\Sigma = P_i^{\text{RH}}$, μ_Σ is the radio-head efficiency [10]. The throughput of the system is defined as $R_{\text{FAP},i} = M/T_{\text{FAP}}^{\text{RH},i}$, which is greater or equal to the offered load: $R_{\text{traffic}} = M/T_{\text{FAP}}^{\text{OH}}$. The term $\frac{P_i^{\text{RH}}}{R_{\text{FAP},i}}$ in (8) is an indication of the average radio transmission efficiency, which does not consider the overhead energy. This is commonly used to measure energy consumption in literature, and is known as the Energy-Consumption-Ratio (ECR).

Fig. 6 shows the ERG performance for the same three sets of equivalent investigation in Fig. 3, Fig. 4 and Fig. 5. Approximately 8% of OP energy can be saved when the source of the interference is close to the FAP (150 m), and 1% OP energy reduction can be made when the interference source is far from the FAP (450 m). The reason being that in the latter case, no matter where the FAP is located, all user locations in the room will experience a saturated throughput. Thus, the challenge of optimal FAP placement is non-existent. In terms of the global context, there are 1 billion people in developed countries and if each house with 5 people has 1 FAP of a persistent 10 W operational power consumption, the annual

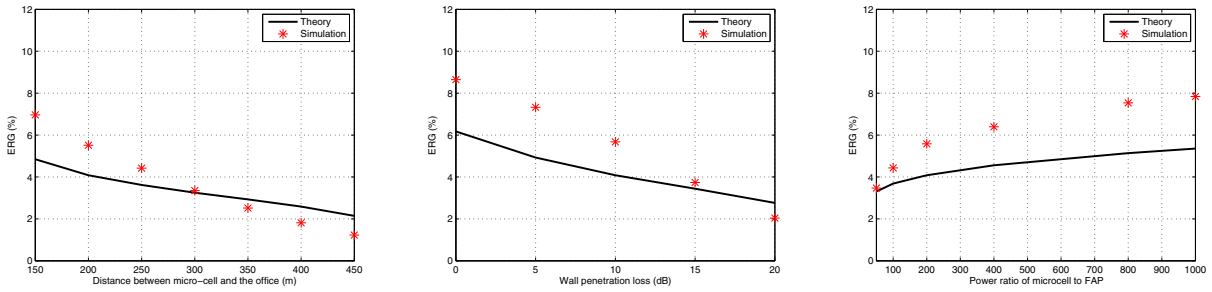

(a) Impact of distance between micro-cell and the office effect

(b) Wall penetration loss effect

(c) Power ratio of microcell to FAP

Fig. 6. Operational Energy Reduction Gain (ERG): Theoretical (line) and simulation (symbols) results of Optimal FAP Placement.

$$
\begin{aligned}
S_1 &= \int_{b+d_{bp2}}^{Y} \log_2(y-b)\ \mathrm{d}y = y\log_2(y-b)\Big|_{b+d_{bp2}}^{Y} - \int_{b+d_{bp2}}^{Y} \frac{y}{(y-b)\ln 2}\ \mathrm{d}y, \\
&= \underbrace{Y\log_2(Y-b) - (b+d_{bp2})\log_2 d_{bp2}}_{=T_1} - \frac{1}{\ln 2}\int_{b+d_{bp2}}^{Y} \frac{y-b+b}{y-b}\ \mathrm{d}y = T_1 - \frac{1}{\ln 2}\left[y + b\ln(y-b)\right]\Big|_{b+d_{bp2}}^{Y}, \\
&= T_1 - \frac{1}{\ln 2}\left[Y - b - d_{bp2} + b\ln(Y-b) - b\ln d_{bp2}\right] = T_1 - \underbrace{\left(\frac{Y-b-d_{bp2}}{\ln 2} + b\log_2\frac{Y-b}{d_{bp2}}\right)}_{U_1}.
\end{aligned}
\tag{9}
$$

electricity energy consumed is 17–20 TWh (10^{12} W). This is a lower bound as those duplicate FAPs in un-developed nations, shops, outdoors and workplace is not considered. With the optimal FAP placement, 1.6 TWh can be saved, which translates to the power generated by two 1000 MW power plants.

V. Conclusions

In this paper, a theoretical and simulation optimisation framework has been proposed to find the optimal placement of an indoor femtocell access point in the presence of a macro-cell interference source. The framework takes into account propagation parameters, transmitting power levels, mutual information saturation, and the relative position of the indoor room with respect to the outdoor cell-site. This work can be extended to consider multiple FAPs and outdoor cells. The comparison between theory and simulation shows a good agreement, which indicates that the theoretical model can yield useful insights into the interaction between FAP location and performance. The key result is that the optimal FAP position varies between the centre of the room to towards the interfering BS, depending on the scenario. Compared to the conventional FAP placement, a performance improvement of up to 20% in mean capacity and an 8% reduction in operational energy reduction has been achieved. Given the large number of indoor access points in the world, this leads to a significant world-wide energy reduction.

Appendix

It is important to note that due to capacity saturation, the mean capacity of the indoor users has to be broken up into the following 3 scenarios:

1) Scenario 1: the FAP is close to the window ($0 < b \leq b_1$) so that the only non-saturated capacity region is away towards the wall.
2) Scenario 2: the FAP is in the middle region of the room ($b_1 < b \leq b_2$) so that the non-saturated capacity regions exist both towards the window and the wall.
3) Scenario 3: the FAP is close to the far wall ($b_2 < b \leq Y$) so that the only non-saturated capacity region is towards the window.

We now consider these scenarios in turn and combine their theoretical formulation.

A. Formulation Scenario 1

In the **first scenario**, the farthest coordinate for FAP cannot exceed b_1 where the SINR value at the wall close to the micro-cell side (i.e. $d_{x,y,\mathrm{in}} = 0$) should just achieve the saturation SNR threshold γ_s. Hence, b_1 can be calculated as:

$$
K_\gamma \frac{10^{\beta d_{y,\mathrm{in}}}}{b_1^\alpha} = 10^{\frac{\gamma_s}{10}}, \Rightarrow b_1 = \sqrt[\alpha]{\frac{K_\gamma}{10^{\frac{\gamma_s}{10}}}} \tag{10}
$$

The capacity can therefore be expressed by:

$$\begin{aligned}\overline{C}_1^b &= \frac{1}{Y}\int_0^{b+d_{bp2}} C_{\mathrm{s}}\ \mathrm{d}y + \frac{1}{Y}\int_{b+d_{bp2}}^{Y} \log_2\left[K_\gamma \frac{10^{\beta y}}{(y-b)^\alpha}\right]\ \mathrm{d}y,\\ &= \underbrace{\frac{(b+d_{bp2})C_{\mathrm{s}}}{Y}}_{=P_1} + \underbrace{\frac{(Y-b-d_{bp2})\log_2 K_\gamma}{Y}}_{=Q_1}\\ &+ \frac{\beta\log_2 10}{Y}\int_{b+d_{bp2}}^{Y} y\ \mathrm{d}y - \frac{\alpha}{Y}\overbrace{\int_{b+d_{bp2}}^{Y}\log_2(y-b)\ \mathrm{d}y}^{=S_1},\\ &= P_1 + Q_1 + \underbrace{\frac{\beta\log_2 10}{2Y}[Y^2-(b+d_{bp2})^2]}_{=R_1} - \frac{\alpha}{Y}S_1.\end{aligned} \tag{11}$$

The term d_{bp2} can be solved by the following equation:

$$K_\gamma \frac{10^{\beta(b+d_{bp2})}}{d_{bp2}^\alpha} = 10^{\frac{\gamma_s}{10}}, \Rightarrow d_{bp2} = B\exp\left[-W\left(-F\right)\right], \tag{12}$$

where $B = 10^{\frac{b}{20\alpha}}\left(\frac{K_\gamma}{\frac{\gamma_s}{10^{10}}}\right)^{\frac{1}{\alpha}}$, $F = \frac{\ln 10}{20\alpha}B$, W is ***Lambert W*** function, namely the branches of the inverse relation of the function $f(W) = W\exp(W)$. S_1 can then be calculated in (9).

By substituting Eq. (9) for S_1 in Eq. (11), $\overline{C}_1^b$ can be finalised as:

$$\overline{C}_1^b = P_1 + Q_1 + R_1 - \frac{\alpha}{Y}(T_1 - U_1). \tag{13}$$

B. Formulation Scenario 2

When the position of FAP is on the coordinate b_2, the user's SINR at the other end of the office is equal to γ_s. b_2 needs to be determined before assigning the proper limits for the mean capacity integral. With reference to Eq. (10), b_2 can be found to be:

$$b_2 = Y - \sqrt[\alpha]{\frac{K_\gamma 10^{\beta Y}}{10^{\frac{\gamma_s}{10}}}}. \tag{14}$$

After b_2 is solved, the mean capacity in this scenario can therefore be expressed by:

$$\begin{aligned}\overline{C}_2^b &= \frac{1}{Y}\int_0^{b-d_{bp1}} \log_2\left[K_\gamma\frac{10^{\beta y}}{(b-y)^\alpha}\right]\ \mathrm{d}y + \frac{1}{Y}\int_{b-d_{bp1}}^{b+d_{bp2}} C_{\mathrm{s}}\ \mathrm{d}y\\ &+ \frac{1}{Y}\int_{b+d_{bp2}}^{Y}\log_2\left[K_\gamma\frac{10^{\beta y}}{(y-b)^\alpha}\right]\ \mathrm{d}y,\\ &= P_2 + Q_2 + R_1 + R_2 - \frac{\alpha}{Y}(T_1 + T_2 - U_1 - U_2),\end{aligned} \tag{15}$$

where d_{bp1} can be solved by the following equation:

$$K_\gamma\frac{10^{\beta(b-d_{bp1})}}{d_{bp1}^\alpha} = 10^{\frac{\gamma_s}{10}}, \Rightarrow d_{bp1} = B\exp\left[-W\left(F\right)\right], \tag{16}$$

The notation of other variables are as follows: $P_2 = \frac{(d_{bp1}+d_{bp2})C_{\mathrm{s}}}{Y}$, $Q_2 = \frac{(Y-d_{bp1}-d_{bp2})\log_2 K_\gamma}{Y}$, $R_2 = \frac{\beta\log_2 10}{2Y}(b-d_{bp1})^2$, $T_2 = (b-d_{bp1})\log_2 d_{bp1}$, and $U_2 = \frac{b-d_{bp1}}{\ln 2} + b\log_2\frac{d_{bp1}}{b}$.

C. Formulation Scenario 3

In the last scenario, the mean capacity expression is very similar to that in scenario one and is given by:

$$\begin{aligned}\overline{C}_3^b &= \frac{1}{Y}\int_0^{b-d_{bp1}}\log_2\left[K_\gamma\frac{10^{\beta y}}{(b-y)^\alpha}\right]\ \mathrm{d}y + \frac{1}{Y}\int_{b-d_{bp1}}^{Y} C_{\mathrm{s}}\ \mathrm{d}y,\\ &= P_3 + Q_3 + R_2 - \frac{\alpha}{Y}(T_2 - U_2),\end{aligned} \tag{17}$$

where $P_3 = \frac{(Y-b+d_{bp1})C_{\mathrm{s}}}{Y}$, and $Q_3 = \frac{(b-d_{bp1})\log_2 K_\gamma}{Y}$.

ACKNOWLEDGMENT

The work reported in this paper has formed part of the Green Radio Core 5 Research Programme of the Virtual Centre of Excellence in Mobile and Personal Communications, Mobile VCE. Fully detailed technical reports on this research are available to Industrial Members of the Mobile VCE. http://www.mobilevce.com

REFERENCES

[1] V. Chandrasekhar, J. Andrews, and A. Gatherer, "Femtocell networks: a survey," *Communications Magazine, IEEE*, vol. 46, no. 9, pp. 59–67, 2008.

[2] V. Chandrasekhar, J. Andrews, T. Muharemovic, Z. Shen, and A. Gatherer, "Power control in two-tier femtocell networks," *Wireless Communications, IEEE Transactions on*, vol. 8, no. 8, pp. 4316–4328, 2009.

[3] H. Jo, C. Mun, J. Moon, and J. Yook, "Interference mitigation using uplink power control for two-tier femtocell networks," *Wireless Communications, IEEE Transactions on*, vol. 8, no. 10, pp. 4906–4910, 2009.

[4] V. Chandrasekhar and J. Andrews, "Uplink capacity and interference avoidance for two-tier femtocell networks," *Wireless Communications, IEEE Transactions on*, vol. 8, no. 7, pp. 3498–3509, 2009.

[5] D. Fagen, P. Vicharelli, and J. Weitzen, "Automated wireless coverage optimization with controlled overlap," *Vehicular Technology, IEEE Transactions on*, vol. 57, no. 4, pp. 2395–2403, 2008.

[6] I. Ashraf, H. Claussen, and L. Ho, "Distributed radio coverage optimization in enterprise femtocell networks," in *Communications (ICC), 2010 IEEE International Conference on*. IEEE, pp. 1–6.

[7] J. Torregoza, R. Enkhbat, and W. Hwang, "Joint power control, base station assignment, and channel assignment in cognitive femtocell networks," *EURASIP Journal on Wireless Communications and Networking*, vol. 2010, p. 6, 2010.

[8] P. Kyösti, J. Meinilä, L. Hentilä, X. Zhao, T. Jämsä, C. Schneider, M. Narandzic, M. Milojevic, A. Hong, J. Ylitalo *et al.*, "WINNER II channel models (d1. 1.2 v1. 1)," *no. IST-4-027756 WINNER II, D*, vol. 1.

[9] C. Mehlüfuhrer, M. Wrulich, J. Ikuno, D. Bosanska, and M. Rupp, "Simulating the Long Term Evolution physical layer," in *Proc. of the 17th European Signal Processing Conference (EUSIPCO 2009), Glasgow, Scotland*, 2009.

[10] EARTH, "Energy efficiency analysis of the reference systems, areas of improvements and target breakdown," Energy Aware Radio and neTwork tecHnologies, Tech. Rep. Deliverable D2.3, December 2010.